# Effect of Processing Conditions on Crystallization Kinetics of a Milk Fat Model System

**M.L. Herrera and R.W. Hartel***

Department of Food Science, University of Wisconsin-Madison, Madison, Wisconsin 53706

**ABSTRACT:** Crystallization behavior of three blends of 30, 40, and 50% of high-melting fraction (MDP = 47.5°C) in low-melting fraction (MDP = 16.5°C) of milk fat was studied under dynamic conditions in laboratory scale. The effect of cooling and agitation rates, crystallization temperature, and chemical composition of the blends on the morphology, crystal size distribution, crystal thermal behavior, polymorphism, and crystalline chemical composition was investigated by light microscopy, differential scanning calorimetry (DSC), X-ray diffraction (XRD) and gas chromatography (GC). Different nucleation and growth behavior were found for different cooling rates. At slow cooling rate, larger crystals were formed, whereas at fast cooling rate, smaller crystals appeared together. Slowly crystallized samples had a broader distribution of crystal size. Crystallization temperatures had a similar effect as cooling rate. At higher crystallization temperatures, larger crystals and a broader crystal size distribution were found. Agitation rate had a marked effect on crystal size. Higher agitation rates lead to smaller crystal size. Cooling rate was the most influential parameter in crystal thermal behavior and composition. Slowly crystallized samples showed a broader melting diagram and an enrichment of long-chain triacylglycerols. Crystallization behavior was more related to processing conditions than to chemical composition of blends.

Paper no. J9182 in *JAOCS 77*, 1177–1187 (November 2000).

**KEY WORDS:** Crystal morphology, crystal size distribution, growth, milk fat fractions blends, nucleation, processing conditions, polymorphism, thermal behavior.

---

The crystallization process may be separated into two steps: nucleation and crystal growth. However, both events often occur simultaneously, making it difficult to determine kinetics for each process (1). Yet, kinetics of crystallization is important for controlling operations in the food industry to produce the desired product characteristics. For a natural lipid to crystallize, it must be supersaturated or supercooled to provide a driving force for both crystallization steps (2). The kinetics of crystallization in lipids is dependent on the triacylglycerol (TAG) composition, the level of minor components, and processing conditions (temperature, cooling rate, agitation rate, etc.).

Milk fat has a heterogeneous nature. It contains a large variety of fatty acids with different chain lengths. The crystallization and melting behaviors of milk fat are dictated by its inherent chemical composition and are influenced by the conditions employed during processing. Parameters such as crystallization rate and temperature employed during processing can have a marked effect on the physical properties of milk fat. The crystallization temperature affects the formation of the various polymorphs, the size of the crystals, composition of the solid fat, and the physical properties of the fractions (3–6). The effects of cooling rates were examined by deMan (7) and Schaap and Rutten (6), who found little difference in slip point, solid fat content (SFC), yield, hardness, thermal melting curves, and fatty acid composition over the range from 0.01 to 1°C/min. However, Deffense (8) reported that the process parameters during crystallization must be controlled to achieve the desired crystalline properties. The chemical composition of fractions obtained by dry fractionation of milk fat was dependent on crystallization rate and initial fat composition (8). Grall and Hartel (9) quantified the effects of various operating parameters on the crystallization kinetics of butterfat. They proposed different mechanisms for growth at different crystallization temperatures.

The range of melting properties available from milk fat fractions provides an opportunity to blend intact milk fat and milk fat fractions systematically to create ingredients with selected melting profiles. The blending of fractions gives a manufacturer greater flexibility to tailor milk fat ingredients to specific functional requirements than could be accomplished with fractionation alone. However, the complex interactions that occur when fractions are blended with each other and with other fats are not fully understood. Therefore, greater knowledge of the effects of blending on the melting properties and crystallization behavior of milk fat fractions would enhance the capacity to accurately predict the functionality of milk fat ingredients made from milk fat fractions with known physical and chemical characteristics (10).

The aim of this work was to study the effects of processing conditions on the kinetics of crystal formation and growth in blends of milk fat fractions. The effects of cooling and agitation rates, crystallization temperature, and initial composition of blends were investigated.

*To whom correspondence should be addressed at 1605 Linden Dr., Madison, WI 53706. E-mail: hartel@calshp.cals.wisc.edu

## MATERIALS AND METHODS

*Starting blends.* Three model systems were prepared by mixing 30, 40, and 50% of high-melting fraction with low-melting fraction of milk fat. Fractions were obtained from Grassland Dairy (Greenwood, WI). The Mettler dropping points (MDP) and TAG composition of the milk fat fractions are reported in Table 1, which also includes MDP and TAG composition of the blends.

*Crystallization procedure.* Samples (500 g) were melted in a water bath at 80°C and kept at this temperature for 40 min. The melted samples were placed in a 1.0-L stainless-steel jacketed vessel with a 23-cm height and an 8.4-cm inner diameter. A mixer was attached to a Master Servodyne (Servodyne Controller, Chicago, IL) drive unit, which maintained constant motor speed. The mixer consisted of a 0.8-cm diameter and 39.2-cm length polypropylene shaft with a U-shaped blade paddle assembly for mixing highly viscous liquids. Maximum paddle diameter was 6.6 cm. A copper-constantan thermocouple, attached to an aluminum brace and positioned 1 cm from the center of the tank and 2 cm from the top of the sample, was used to determine sample temperature. Bath and sample temperatures were recorded. Samples were cooled at two rates. For the fast rate, a Lauda RC 20 (Lauda, Königshofen, Germany) water bath was set at crystallization temperatures of 25, 27.5, and 30°C. Cooling rate was calculated from the slope of the linear part of sample temperature profile (reported in Table 2). For the slow cooling rate, the set point temperature of the Lauda water bath was reduced to the same crystallization temperatures at a rate of 1°C every 5 min. Constant agitation rates of 50, 100, 150, 200, and 300 rpm were used. All the experiments were run in duplicate and results were averaged.

*Light microscopy.* Sample collection began when the crystallizer temperature reached 37°C, continued as temperature fell to crystallization temperature and up to 2 h after crystallization heat was noticed. At each sample point, a drop of slurry was placed between a warmed slide and a cover slide. Crystals were observed with a polarized-light microscope (Nikon Optiphot, Garden City, NY) equipped with a video camera connected to a computer. Optimas 6.1 (Optimas, Bothell, WA) software was used to collect the images. Images were taken in duplicate at every sample time with a 10× objective and a television relay ocular lens. After 2 h, the crystallization process was almost complete, based on preliminary experiments that documented that SFC reached over 95% of the equilibrium SFC at these crystallization temperatures. At that time, 1 mL of slurry from the crystallizer was diluted with a drop of butanol to disperse the crystals for image analysis and at least 20 images were taken. The individual crystal areas were measured using the Optimas software, and the results were exported to Microsoft Excel 7.0 (Microsoft, Redmond, WA) software for graphic presentation of data. Between 200 and 300 crystals were measured for each sample. The diameters of circles having equivalent areas to the measured areas were reported.

**TABLE 1**
**Mettler Dropping Points and Triacylglycerol Composition of Milk Fat Fractions and Their Blends[a]**

| TAG carbon number | Milk fat | HMF | LMF | 30–70% HMF/ LMF | 40–60% HMF/ LMF | 50–50% HMF/ LMF |
|---|---|---|---|---|---|---|
| 28 | 0.8 | — | 0.8 | 0.6 | 0.7 | 0.5 |
| 30 | 1.2 | 0.7 | 1.5 | 1.1 | 1.2 | 1.0 |
| 32 | 2.5 | 1.4 | 2.9 | 2.4 | 2.4 | 2.0 |
| 34 | 4.5 | 3.2 | 6.2 | 5.1 | 5.1 | 4.3 |
| 36 | 9.4 | 5.9 | 11.1 | 8.9 | 8.8 | 8.1 |
| 38 | 13.3 | 9.5 | 14.5 | 12.0 | 14.4 | 10.8 |
| 40 | 11.0 | 6.6 | 12.7 | 10.7 | 9.4 | 9.2 |
| 42 | 7.0 | 5.6 | 6.8 | 6.4 | 6.1 | 6.1 |
| 44 | 6.2 | 6.8 | 5.3 | 5.8 | 5.6 | 6.1 |
| 46 | 6.8 | 10.1 | 5.4 | 6.9 | 6.8 | 7.9 |
| 48 | 8.6 | 14.0 | 6.5 | 9.0 | 9.1 | 10.5 |
| 50 | 11.5 | 18.3 | 8.7 | 11.9 | 12.1 | 13.6 |
| 52 | 11.5 | 12.1 | 10.8 | 12.2 | 12.0 | 13.0 |
| 54 | 5.7 | 5.8 | 6.7 | 6.5 | 5.4 | 6.4 |
| MDP | 34.5 | 47.6 | 16.7 | 38.0 | 40.5 | 42.2 |

[a]TAG, triacylglycerol; HMF, high-melting fraction; LMF, low-melting fraction; MDP, Mettler dropping point (°C).

**TABLE 2**
**Cooling Data for the 50—50% Blend of High-Melting in Low-Melting Milk Fat Fractions Crystallized at 25¡C**

| Agitation rate (rpm) | Cooling rate (ºC/min) | Rising temperature[a] (ºC) | Time[b] (min) |
|---|---|---|---|
| 50 | 5.3 | 29.6 | 4 |
| | 0.2 | 34.8 | 9 |
| 100 | 5.5 | 28.6 | 4 |
| | 0.2 | 34.1 | 9 |
| 150 | 5.5 | 29.3 | 5 |
| | 0.2 | 34.5 | 10 |
| 200 | 5.3 | 27.8 | 2 |
| | 0.2 | 35.0 | 12 |
| 300 | 5.5 | 27.8 | 2 |
| | 0.2 | 35.5 | 9 |

[a]Temperature at which latent heat started to be noticeable.
[b]Time during which sample temperature did not follow bath temperature.

*Nuclear magnetic resonance (NMR).* SFC of the samples were measured by pulsed NMR (pNMR) in a Minispec PC/120 series NMR analyzer (Bruker, Karlsruhe, Germany). Samples were run in duplicate and the values were averaged. The actual SFC was determined 20 and 80 min after sample reached crystallization temperature.

After 2 h of crystallization, samples were vacuum-filtered at crystallization temperature, and the crystals remaining on the filter paper were analyzed for their thermal behavior by differential scanning calorimetry (DSC), polymorphism by X-ray diffraction (XRD), and chemical composition by gas chromatography (GC).

*DSC.* Thermograms were obtained with a Pyris 1 Perkin-Elmer calorimeter (PerkinElmer, Chicago, IL) and Pyris™ software for Windows. The DSC was calibrated with indium and mercury standards prior to analysis. Dry nitrogen gas was used to purge the thermal analysis system, and a mechanical

cooler was used to cool the system. Samples (5–15 mg) were sealed into aluminum pans (TA Instruments, New Castle, DE) and placed in the DSC. Changes in heat flow during melting were recorded. The following temperature protocol was used: –10°C for 1 min and heat to 80°C at a rate of 5°C/min.

*XRD.* Short spacings were measured by means of a Nicolet 12v powder X-ray diffractometer (Nicolet, Madison, WI) equipped with graphite-monochromated Cu $K_\alpha$ radiation ($\gamma$ = 0.1542 nm). A 2θ scan from 5 to 30 at a scanning velocity of 1°/min was performed at ambient temperature.

*GC.* Acyl carbon profile was determined using a Hewlett-Packard 5890 Series II (Hewlett-Packard, San Fernando, CA) GC unit equipped with a flame-ionization detector (FID) and on-column injector. The column used was a Heliflex Phase AT-1 with a length of 30 m and an internal diameter of 0.25 mm (Alltech Associates, Deerfield, IL). Helium was the carrier gas at a flow rate of 2 mL/min with hydrogen gas and air also being supplied to the FID. Samples were prepared by using a modified method of Lund (11). Each sample (10 mg) was weighed into a GC vial and dissolved in 1.8 mL of isooctane, with 100 µL of internal standard ($C_{27}$ in isooctane: 2.02 mg/mL) added to the vial. Samples were stored in a refrigerator prior to analysis. To separate the different TAG according to acyl carbon number, the following temperature profile was used: initially hold at 280°C for 1 min, and then increase at a rate of 3.0°C/min until a temperature of 355°C was reached. The detector was held constant at 370°C. Composition was based on the area integrated by using ChemStation Chromatography software by Hewlett-Packard. Samples were run in duplicate.

## RESULTS AND DISCUSSION

*Processing conditions.* To investigate how processing conditions influence crystallization kinetics, the blends were crystallized in a vessel under dynamic conditions. Figure 1 shows characteristic temperature profiles, for slow and fast rates of cooling. Temperature profiles for slow cooling began to deviate slightly from the water bath profile at a certain temperature due to the generation of heat of crystallization. After a short period of deviation from water bath temperature, the sample temperature then followed bath temperature very closely again. In general, when samples were cooled slowly to all selected temperatures and for all agitation rates, sample temperatures did not increase. The release of latent heat was slow and occurred over longer times, as compared to rapid cooling. When samples were cooled rapidly, there was a point where the sample temperature increased by up to 2°C due to the rapid release of latent heat of crystallization. The duration of this temperature increase was about 3 to 5 min, after which the temperature again decreased and followed the water bath profile very closely.

Table 2 shows the temperature at which the crystallization process produced enough heat to be noticeable (called the rising temperature) and the time during which sample temperature rose or did not follow the water bath for the 50–50% blend crystallized to 25°C at all cooling and agitation rates. Average rising temperature for the slow cooling rate was 34.8°C and 28.6°C for fast rate. The point at which the sample temperature did not follow the bath temperature was at least 4.8°C higher for slow cooling than for fast cooling in all cases. In slowly cooled samples, the TAG had more time to interact with each other and, because the cooling time was longer, they crystallized at higher temperatures. Crystallization began at lower temperatures for the fast cooling case, which means these samples crystallized at higher supercoolings. Agitation rate did not influence the point at which temperature rose during cooling to the same extent as cooling rate (Table 2); however, it had a significant influence on the time of deviation of sample temperature from bath temperature (rising time). Rapid agitation rates caused the largest differences in rising time between cooling rates in all cases.

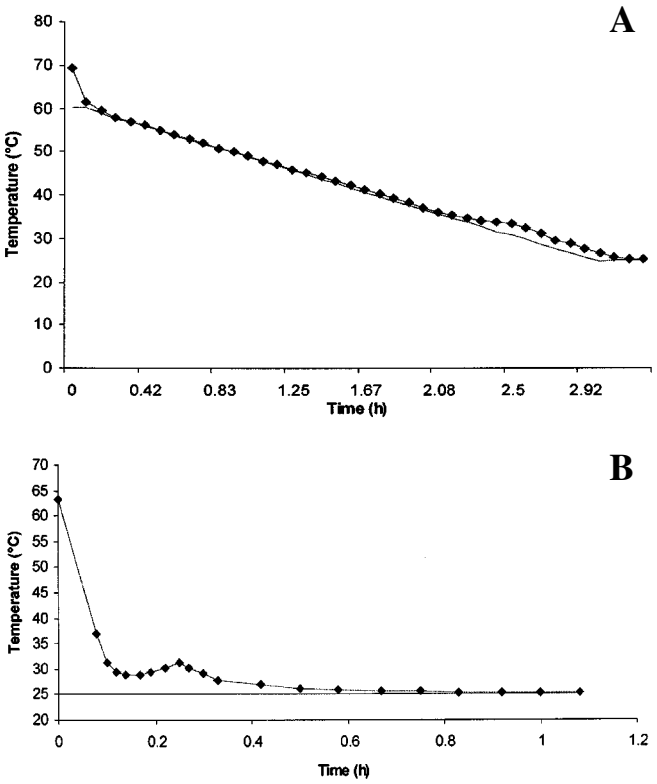


**FIG. 1.** Temperature profiles of water bath (–) and sample (◆) for slow (A) and rapid (B) cooling (50–50% blend crystallized at 25°C and 50 rpm).

*Crystal formation.* To better understand the processes of nucleation and growth under these conditions, samples were taken from the vessel periodically beginning when the temperature reached 37°C and continuing until crystallization temperature was reached. As an example, Figure 2 shows how the crystal images changed for the 30–70% blend crystallized at a slow cooling rate. In each case, slowly crystallized samples showed similar behavior. For the example in Figure 2, sample temperature deviated from the bath temperature at 31.2°C and, as can be observed, nucleation had started before this temperature was reached. At first, only a

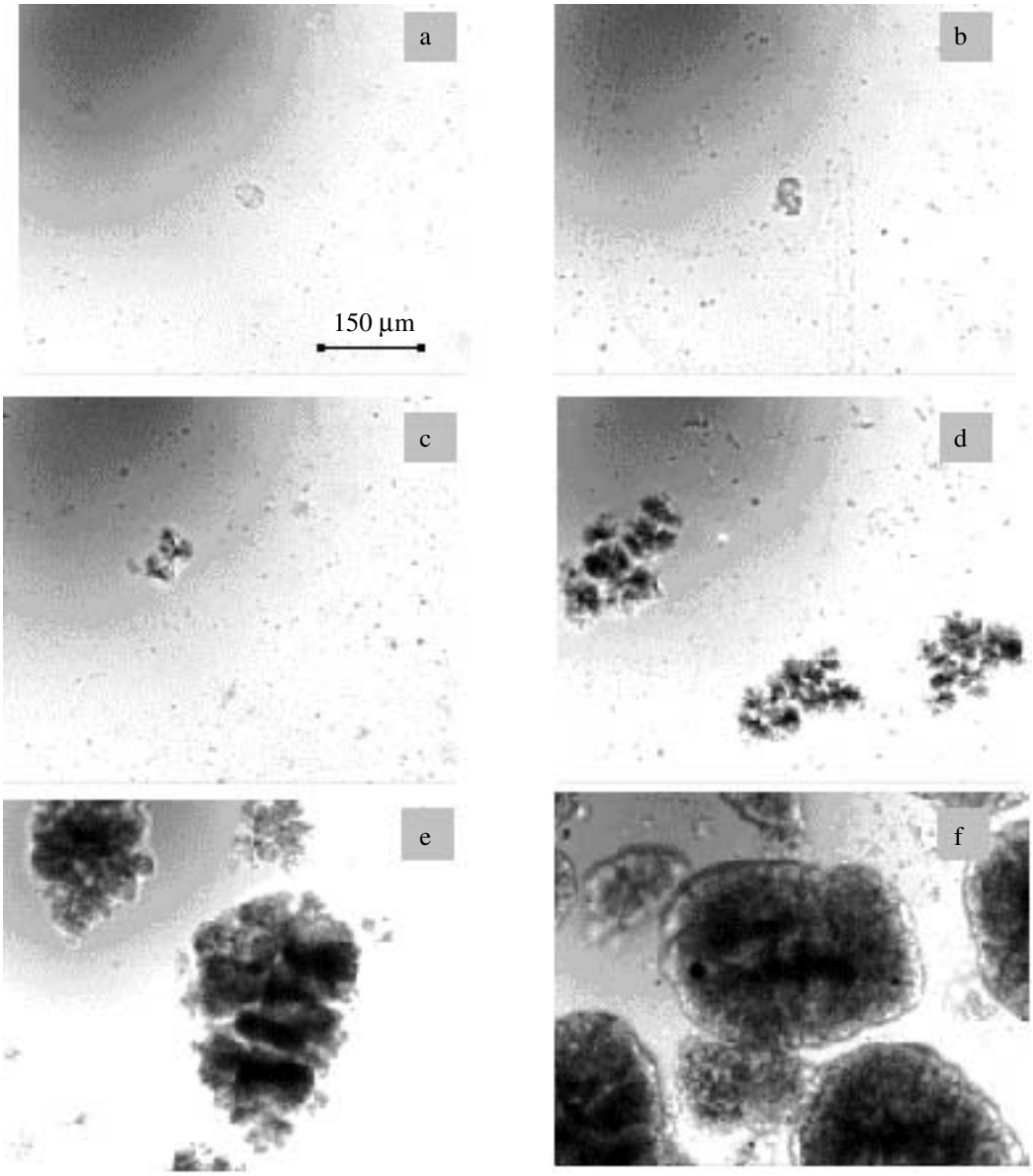


**FIG. 2.** Images of crystals corresponding to a 30–70% blend of high-melting in low-melting milk fat fractions slowly cooled (0.2°C/min) with an agitation rate of 100 rpm. Images were taken at (a) 33.9°C, (b) 33.2°C, (c) 31.9°C, (d) 31.0°C, (e) 28.1°C, and (f) 27.0°C.

few crystals were formed, which grew and caused a release of latent heat. At the same time, new crystals were formed and, as can be observed in the last image in Figure 2, crystals with different size and density (related to opacity of the crystals) were obtained. Figure 3 shows a similar example for the fast cooling rate. When the temperature started to rise (Fig. 3b), numerous crystals had just formed. As these grew, a significant amount of heat was produced. Nucleation and growth continued together and, after 1 h (Fig. 3f) numerous small crystals were obtained. Small crystals, which nucleated later, can be observed in the background. For all samples, the same behavior was found for fast cooling. Figure 4 shows photomicrographs for the same sample as shown in Figure 3, but in this case, the agitation rate was higher. Increased agitation favored the formation of more and smaller initial crystals. Since our vessel was not a closed system, air bubbles were incorporated at higher agitation rates, which potentially helped to initiate nucleation. The air bubbles appeared as dark spots, typically associated with the crystal surface. Higher agitation rates had a very dramatic effect on crystal size, promoting nucleation and resulting in formation of many small crystals.

Figure 5 shows crystal images from the 50–50% blend collected 2 h after crystallization heat was noticed. At that time, the system was approaching phase volume equilibrium, since at least 98% of the maximal crystal content was crystallized (Table 3). Cooling rate influenced the nature of the crystals

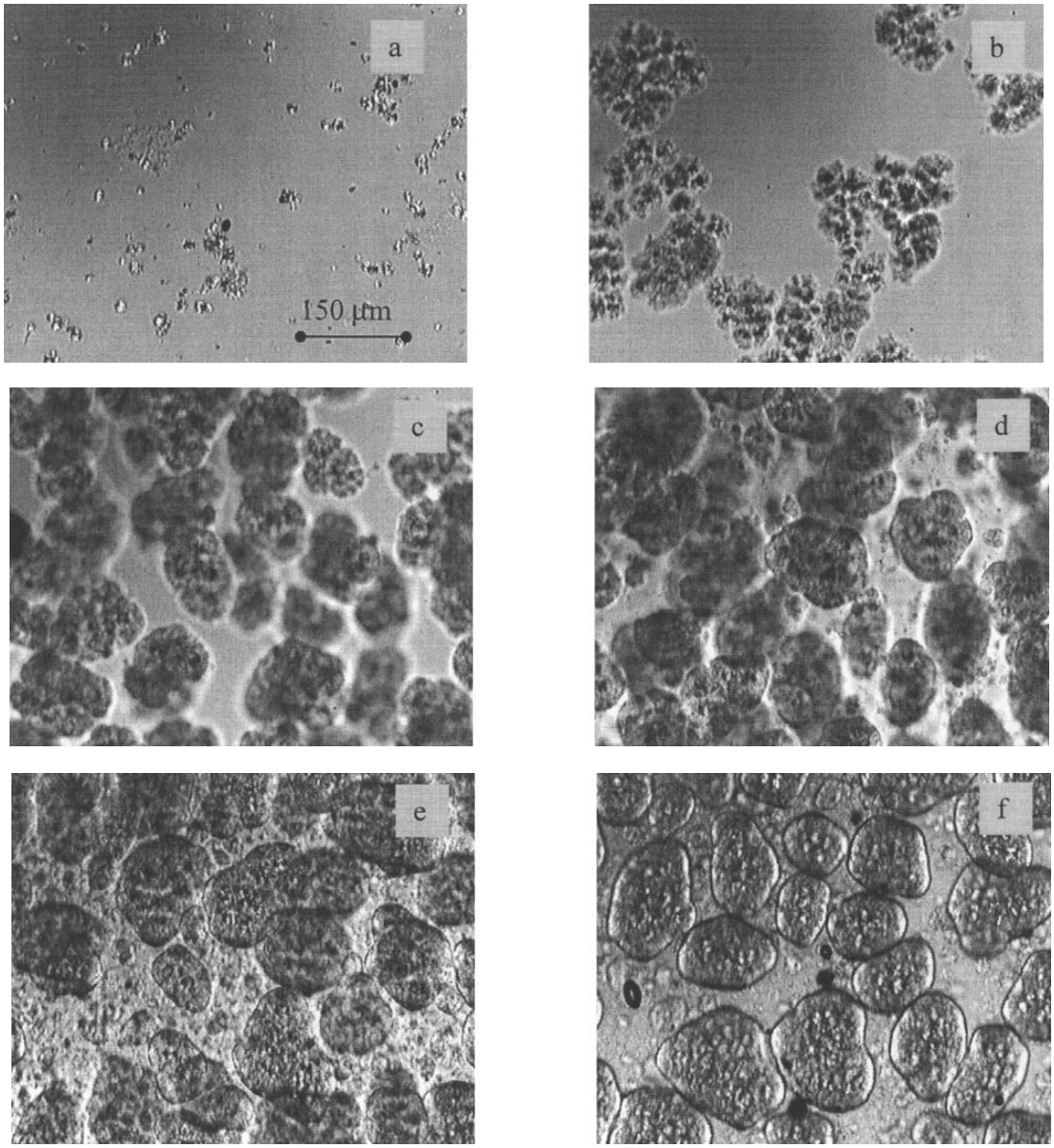


**FIG. 3.** Images of crystals corresponding to a 30–70% blend of high-melting in low-melting milk fat fractions rapidly cooled (5.0°C/min) with an agitation rate of 100 rpm. Images were taken at (a) 25.4°C, (b) 25.8°C, (c) 26.3°C, (d) 26.1°C, (e) 25.4°C, and (f) 25.1°C.

obtained. Slowly crystallized samples appeared to have a denser crystal structure. More solid material was contained in these crystals, and this is why they look darker (more opaque) in the photomicrograph. Rapidly crystallized samples had crystals that were more transparent, with lower amount of solids in each crystal. Agitation produced a marked decrease in crystal size, which was observed at both cooling rates. Similar results were found for all three blends at all conditions studied.

Figure 6 shows the effect of temperature on crystal structure for the 50–50% blend crystallized at a fast cooling rate with an agitation rate of 50 rpm. Crystal morphology was very similar for the three selected crystallization temperatures, but the size increased with temperature. This effect was found in all cases. At higher temperatures, fewer initial crystals were formed and their growth was favored.

The effect of blend composition on crystal structure is shown in Figure 7. The three blends were crystallized slowly at 50 rpm to 25°C. The same kind of crystals were found. The 30–70% blend had bigger crystals since for this sample 25°C is a relatively higher temperature, with a MDP 4°C lower than for the 50–50% blend. In addition to crystal size, the apparent crystal density, seen as darker crystals, increased with the proportion of HMF.

Figure 8 summarizes the effects of formulation and processing conditions on crystal size distribution. Several trends

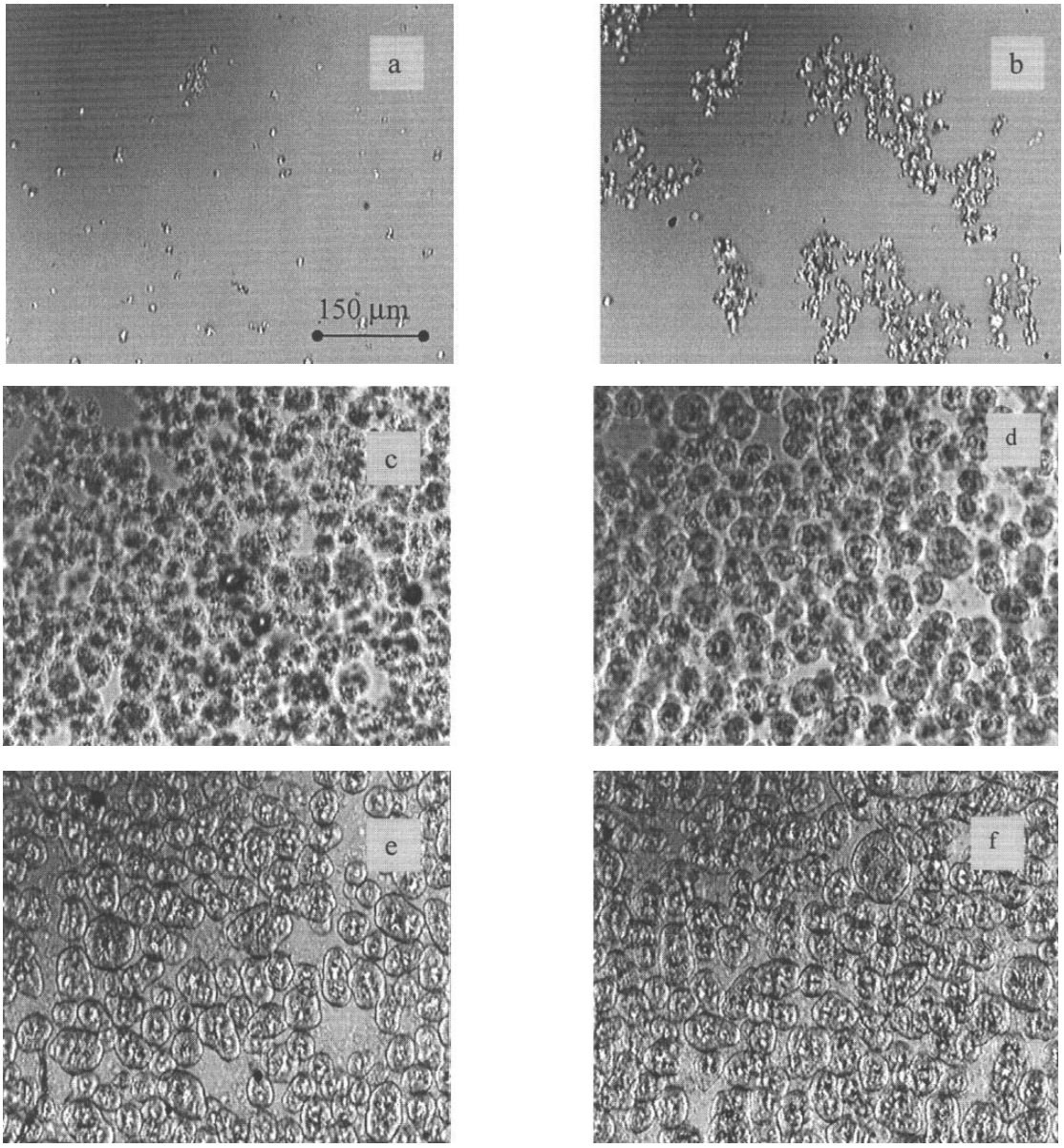


**FIG. 4.** Images of crystals corresponding to a 30–70% blend of high-melting in low-melting milk fat fractions rapidly cooled (5.1°C/min) with an agitation rate of 200 rpm. Images were taken at (a) 26.5°C, (b) 25.7°C, (c) 25.6°C, (d) 26.4°C, (e) 25.4°C, and (f) 25.3°C.

are clear. Slowly crystallized samples showed a broader crystal size distribution than rapidly crystallized samples (c,d). The faster the agitation rate, the smaller the average crystal size (c,f). Average crystal size increased with crystallization temperature (d,e). For the same crystallization temperature, blends with lower MDP had larger average crystal sizes (a,b,c).

*SFC.* Samples were analyzed for their actual SFC at crystallization temperature. Table 3 shows the SFC measured 20 min after the 50–50% blend reached crystallization temperature and 1 h after the first measurement. The 30–70% blend did not show differences in solid content with processing conditions. The other two blends had a slightly lower solid content for slow cooling rate, which was more evident at higher agitation rates. Rapidly cooled samples released latent heat at temperatures more than 4.8°C below those for slowly cooled samples. Thus, rapidly cooled samples were more highly supercooled when crystallization occurred. Fractions crystallized under higher supercooling conditions were reported to have higher SFC because they form compound crystals (12).

*X-ray spectroscopy.* Samples were filtered and the crystals analyzed for polymorphic form. Figure 9 shows two X-ray spectra, which document the effect of cooling rate on the crystals obtained from a 50–50% blend crystallized to 25°C at 200 rpm. Both spectra show characteristic β′ patterns with two strong signals at *d*-spacings of 3.9 and 4.3 Å.

*Chemical composition of crystals.* Table 4 shows the chemical composition of crystals obtained by filtering a 50–50% blend crystallized to 25°C at all cooling and agitation rates used in this

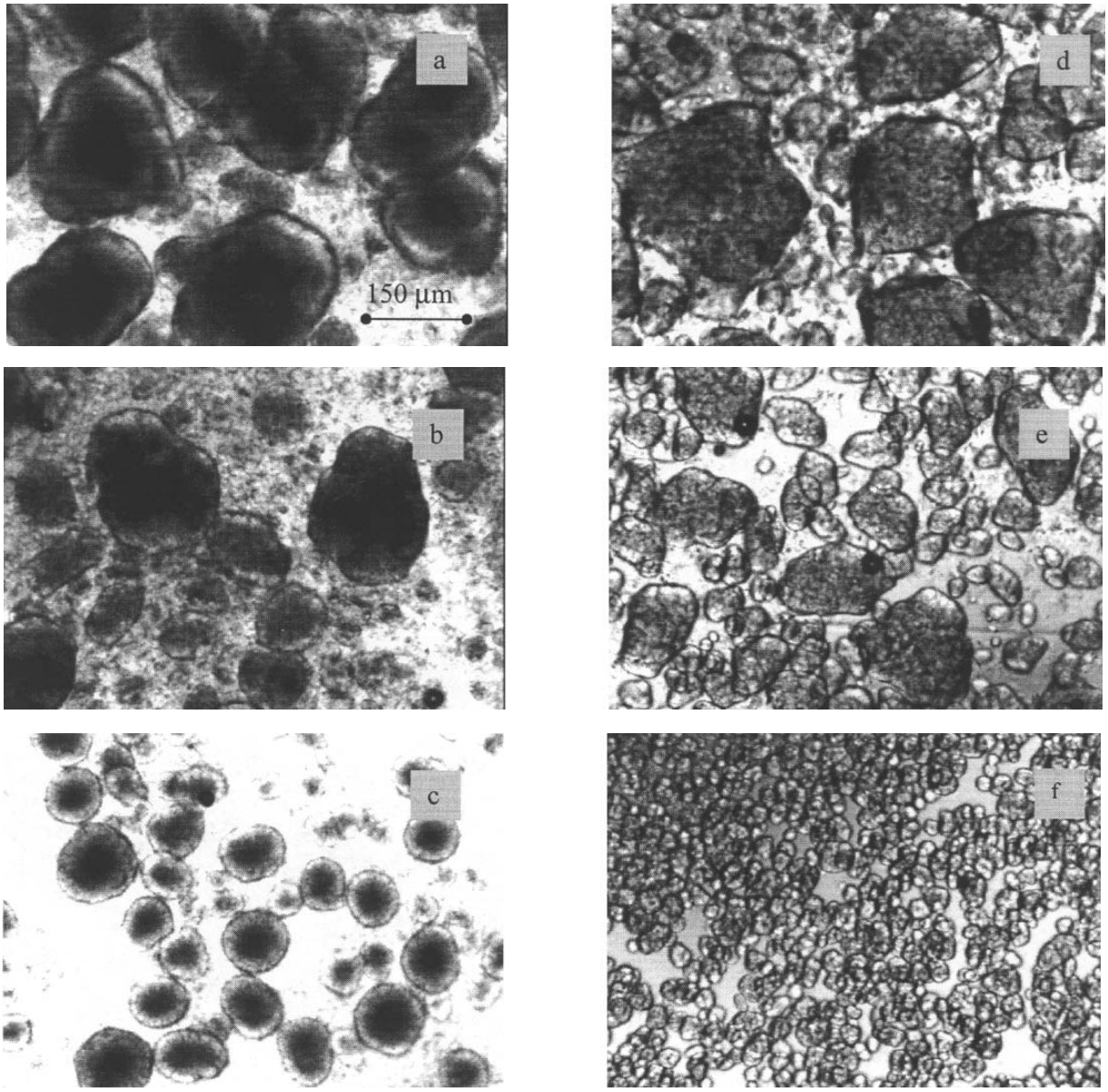


**FIG. 5.** Images of crystals corresponding to a 50–50% blend of high-melting in low-melting milk fat fractions crystallized at 25°C. Samples shown on the left were cooled slowly (0.2°C/min) at (a) 50 rpm, (b) 100, and (c) 200 rpm. Samples shown on the right were cooled rapidly (5.5°C/min) at (d) 50, (e) 100, and (f) 200 rpm.

study. Similar behavior was found for the other blends. Slowly crystallized samples generally had less (0.5 to 2.0 %) TAG with acyl carbon numbers between 32 and 38 and more (0.5 to 3.5%) TAG with acyl carbon numbers from 44 to 50. There were no differences in chemical composition with agitation rates.

*Thermal behavior of crystals.* Figure 10 shows the thermograms of samples corresponding to the X-ray diagrams shown in Figure 9 to document the effect of cooling rate on melting behavior. At slow crystallization rates, the melting temperature range of the main peak was broader; whereas, at fast crystallization rates, a sharper high-melting peak was found. In addition, at the slow cooling rate, high-melting peaks ended at temperatures about 1°C higher. For the example in Figure 10, peak enthalpies were 42.3 and 55.1 J/g for fast and

**TABLE 3**
**Solid Fat Content of the 50—50% Blend of High-Melting in Low-Melting Milk Fat Fractions Crystallized at 25¡C**

| Agitation rate (rpm) | Cooling rate (ºC/min) | Solid fat content after 20 min | Solid fat content after 80 min |
|---|---|---|---|
| 50 | 5.3 | 21.9 | 22.5 |
| | 0.2 | 20.5 | 20.5 |
| 100 | 5.5 | 22.0 | 22.3 |
| | 0.2 | 20.0 | 20.2 |
| 150 | 5.5 | 23.1 | 23.2 |
| | 0.2 | 18.6 | 19.5 |
| 200 | 5.3 | 21.8 | 22.0 |
| | 0.2 | 19.0 | 19.9 |
| 300 | 5.5 | 22.1 | 22.2 |
| | 0.2 | 19.0 | 19.0 |

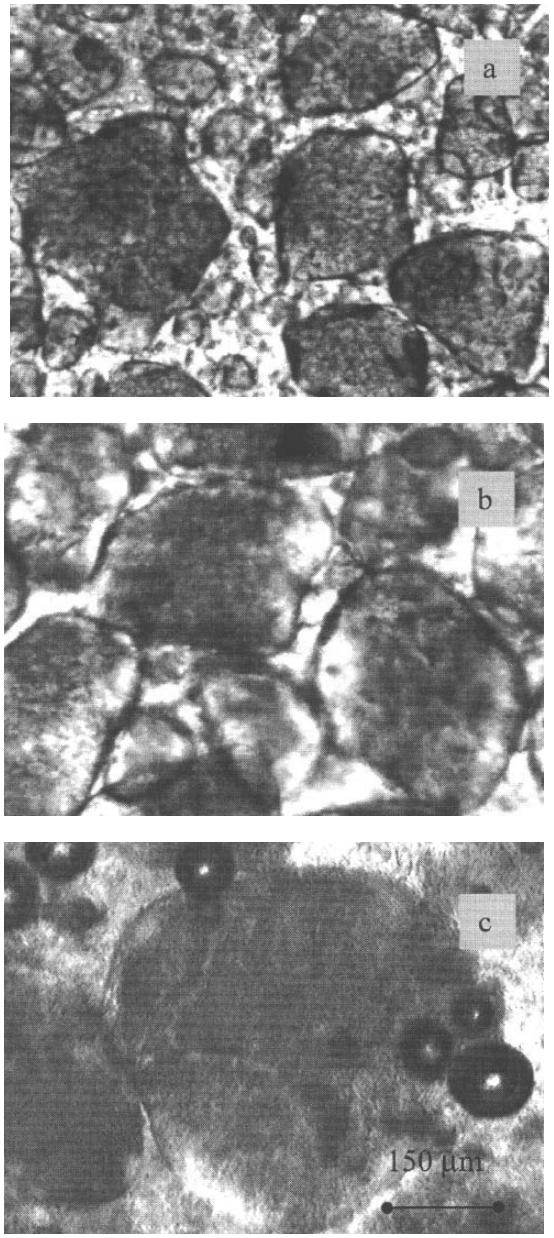


**FIG. 6.** Effect of temperature on crystal size for a 50–50% blend of high-melting in low-melting milk fat fractions rapidly cooled (5.5°C/min) at 50 rpm to (a) 25°C, (b) 27.5°C, and (c) 30°C.

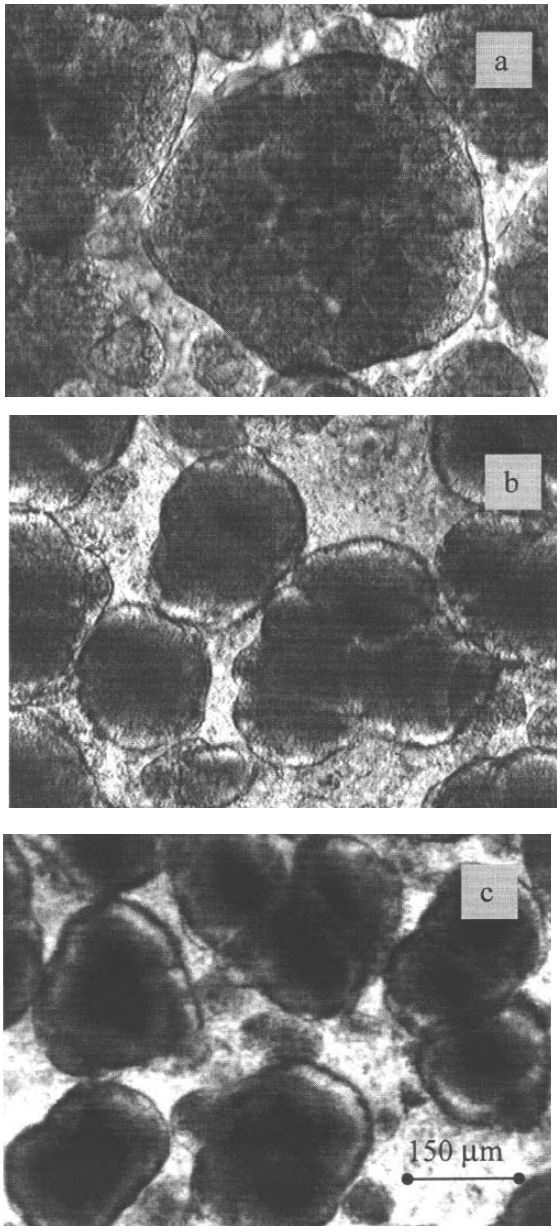


**FIG. 7.** Effect of composition on crystal size and morphology for the blends of high-melting in low-melting milk fat fractions cooled slowly (0.2°C/min) at 50 rpm to 25°C. (a) 30–70%, (b) 40–60%, and (c) 50–50%.

slow cooling rates, respectively. Slowly crystallized samples had slightly higher melting enthalpies in all cases. The higher ending temperatures and enthalpies may be related to the small differences in chemical composition of crystals between cooling rates, particularly the higher content of larger TAG (higher acyl carbon number) (Table 4). However, the broadening at lower temperatures cannot easily be explained by composition since slowly crystallized samples had less of the smaller TAG (lower acyl carbon number). Similar results were found for the effect of cooling rate on melting profiles in hydrogenated sunflower oil, even though there were no observable differences in chemical composition (13,14).

There are two important phenomena that determine the behavior of natural fats: polymorphism and intersolubility (15). In all cases, the β′-form was the major form present and this continued during storage. After 15 d at 10°C, the crystals remained in β′–form. A strong signal at 4.6 Å, typical of transition to the β-form, was not found in the spectra, indicating that polymorphic transition had not yet occurred. However, slightly higher amounts of β-form may have been induced by the slow cooling protocol, as indicated by the shoulder on the X-ray spectra (Fig. 9). Since polymorphic transformation in this stable β′ system is not a main concern, the low-temperature broadening in the DSC curves must be primarily due to the intersolubility of the different TAG components. It has

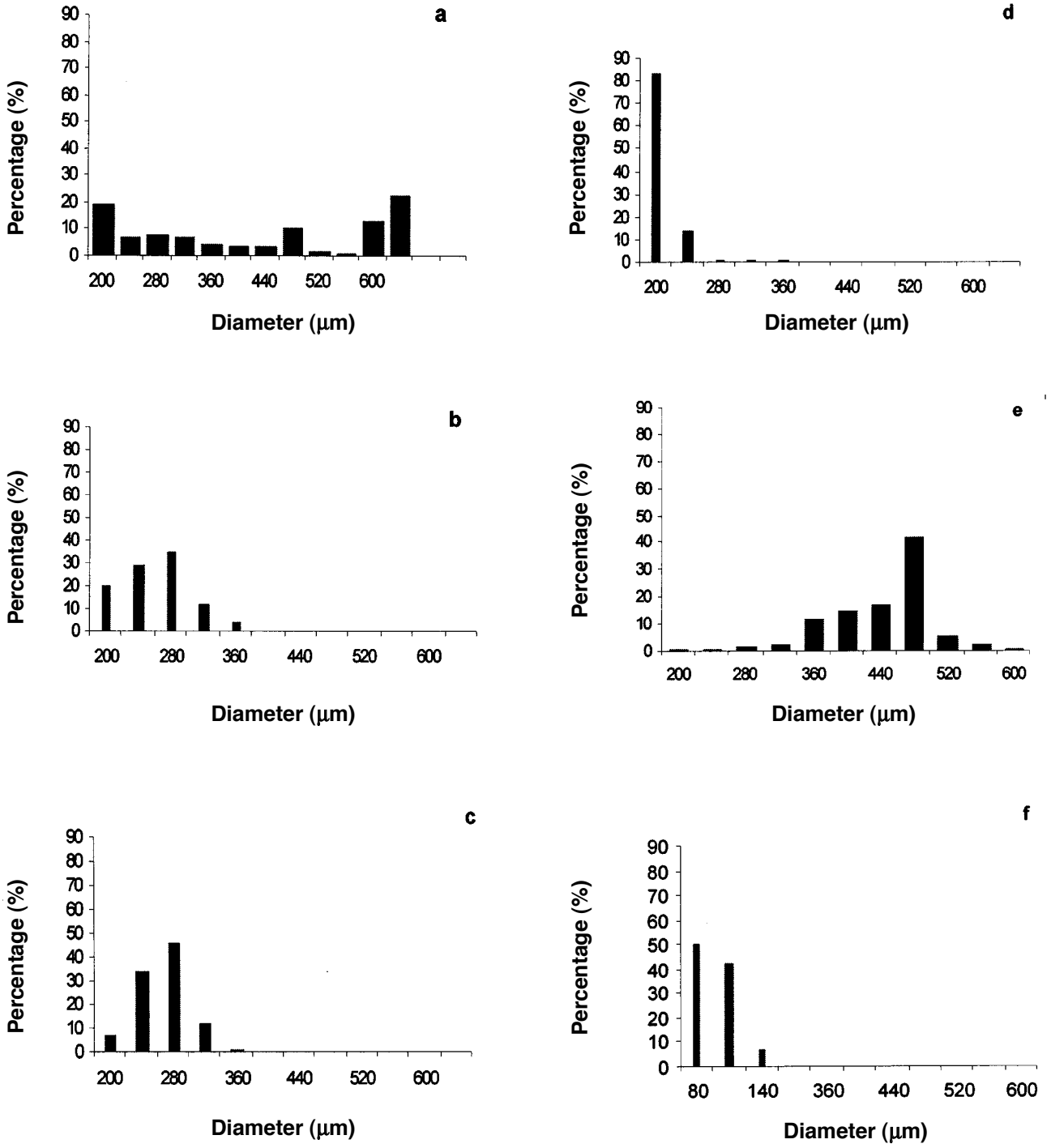


**FIG. 8.** Crystal size distribution of blends of high-melting in low-melting milk fat fractions: (a) 30–70% slowly cooled (0.2°C/min) to 25°C at 50 rpm; (b) 40–60% slowly cooled (0.2°C/min) to 25°C at 50 rpm; (c) 50–50% slowly cooled (0.2°C/min) to 25°C at 50 rpm; (d) 50–50% rapidly cooled (5.5°C/min) to 25°C at 50 rpm; (e) 50–50% rapidly cooled (5.5°C/min) to 30°C at 50 rpm; and (f) 50–50% slowly cooled (0.2°C/min) to 25°C at 200 rpm.

been reported that compound crystals were formed when higher supercooling was attained, even if the supercooling took place only for a short period of time (12). Table 2 shows that rapidly crystallized samples were supercooled at least 4.8 K compared to slowly crystallized samples when crystallization heat was released. These differences in crystallization processes during slow and rapid cooling lead to incorporation of different TAG within the crystal lattice and, thus, different physical properties.

**TABLE 4**
**TAG Composition of the Solid Fractions Obtained from the 50—50% Blend of High-Melting in Low-Melting Milk Fat Fractions Crystallized to 25¡C at All Cooling and Agitation Rates**

| | Agitation rate | | | | | | | | | |
|---|---|---|---|---|---|---|---|---|---|---|
| | 50 | | 100 | | 150 | | 200 | | 300 | |
| | Cooling rate (°C/min) | | | | | | | | | |
| | 5.3 | 0.2 | 5.5 | 0.2 | 5.5 | 0.2 | 5.3 | 0.2 | 5.5 | 0.2 |
| TAG[a] | | | | | | | | | | |
| $C_{28}$ | 0.4 | 0.4 | 0.4 | 0.2 | 0.5 | 0.4 | 0.5 | 0.5 | 0.5 | 0.5 |
| $C_{30}$ | 0.9 | 0.7 | 0.8 | 0.4 | 1.0 | 0.7 | 0.9 | 0.9 | 1.0 | 1.0 |
| $C_{32}$ | 1.9 | 1.2 | 1.8 | 1.4 | 1.9 | 1.6 | 1.8 | 1.6 | 1.8 | 1.3 |
| $C_{34}$ | 4.0 | 3.0 | 3.9 | 3.2 | 4.1 | 3.4 | 3.7 | 3.1 | 3.8 | 1.9 |
| $C_{36}$ | 7.4 | 6.0 | 7.2 | 6.2 | 7.2 | 6.1 | 6.9 | 6.4 | 7.0 | 6.5 |
| $C_{38}$ | 9.9 | 7.7 | 9.3 | 7.5 | 9.8 | 7.7 | 9.6 | 8.8 | 9.7 | 8.1 |
| $C_{40}$ | 8.5 | 6.7 | 8.5 | 7.0 | 9.0 | 8.0 | 8.3 | 8.2 | 8.9 | 8.3 |
| $C_{42}$ | 5.9 | 5.2 | 5.7 | 5.5 | 5.9 | 6.0 | 5.7 | 5.4 | 5.7 | 5.4 |
| $C_{44}$ | 6.3 | 6.4 | 6.3 | 6.5 | 6.2 | 6.0 | 6.3 | 6.2 | 6.1 | 6.6 |
| $C_{46}$ | 8.5 | 9.8 | 8.8 | 9.7 | 8.5 | 9.3 | 8.8 | 9.3 | 8.5 | 9.9 |
| $C_{48}$ | 11.4 | 13.9 | 11.8 | 13.4 | 11.3 | 13.0 | 11.9 | 12.6 | 11.5 | 12.6 |
| $C_{50}$ | 14.9 | 18.4 | 15.4 | 17.6 | 14.8 | 16.5 | 15.4 | 16.4 | 15.0 | 17.0 |
| $C_{52}$ | 13.6 | 14.7 | 13.8 | 15.2 | 13.5 | 14.9 | 13.8 | 14.3 | 14.0 | 14.5 |
| $C_{54}$ | 6.3 | 5.7 | 6.1 | 6.0 | 6.2 | 6.2 | 6.1 | 6.2 | 6.4 | 6.2 |

[a]Acyl carbon number. For abbreviation see Table 1.

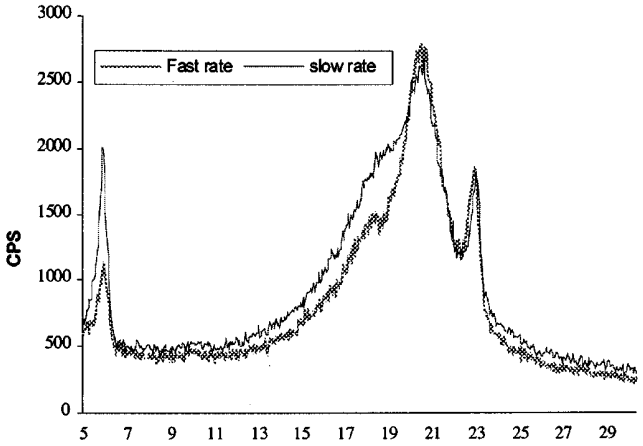


**FIG. 9.** X-ray spectra of a 50–50% blend of high-melting in low-melting milk fat fractions rapidly (5.5°C/min) and slowly (0.2°C/min) cooled at 25°C at 200 rpm.

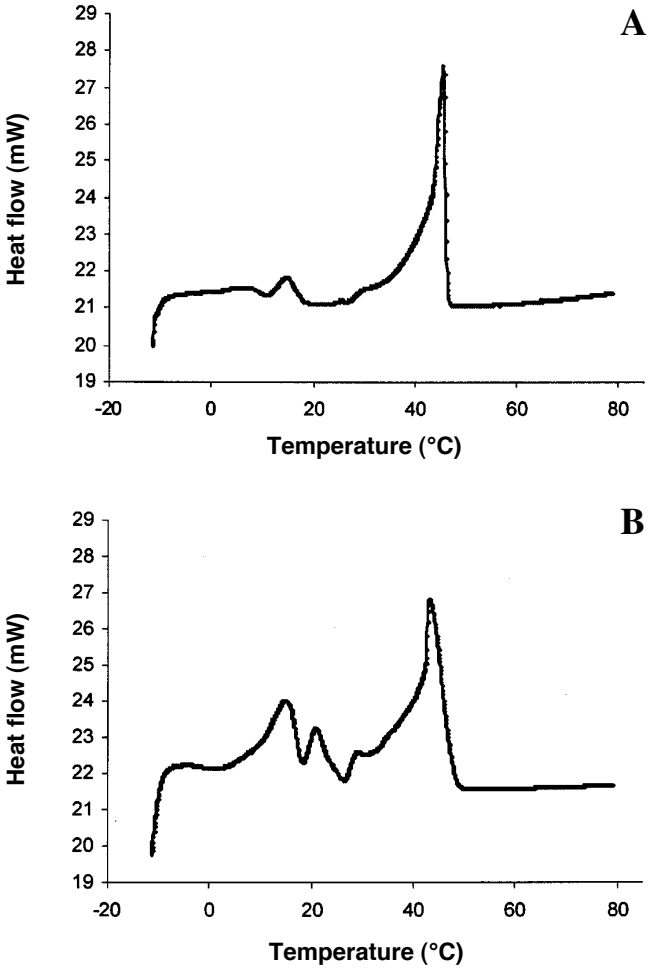


**FIG. 10.** Matching thermograms of the samples corresponding to the X-ray spectra shown in Figure 9; (A) rapid cooling; (B) slow cooling.

## ACKNOWLEDGMENT

To the University of Wisconsin-Madison for its Exchange Visitor Program N° P 1 0105. To the National Research Council of Argentina (CONICET) for the sabbatical granted to Dr. Herrera. Thanks to Professor Alejandro G. Marangoni for his helpful comments throughout the study. This work was funded by the Wisconsin Milk Marketing Board through the Wisconsin Center for Dairy Research.

## REFERENCES

1. Boistelle, R., Fundamentals of Nucleation and Crystal Growth, in *Crystallization and Polymorphism of Fats and Fatty Acids*, edited by N. Garti and K. Sato, Marcel Dekker, Inc., New York, 1988, pp. 189–226.
2. Garside, J., General Principles of Crystallization, in *Food Structure and Behavior*, edited by J.M.V. Blanshard and P. Lillford,

Academic Press, Inc., London, 1987, pp. 35–49.
3. Amer, M.A., D.B. Kupranycz, and B.E. Baker, Physical and Chemical Characteristics of Butterfat Fractions Obtained by Crystallization from Molten Fat, *J. Am. Oil Chem. Soc. 62*:1551–1557 (1985).
4. Antila, V., The Fractionation of Milk Fat, *Milk Industry 81*:17–20 (1979).
5. Foley, J., and J.P. Brady, Temperature-Induced Effects on Crystallization Behavior, Solid Fat Content and the Firmness Values of Milk Fat, *J. Dairy Res. 51*:579–589 (1984).
6. Schaap, J.E., and G.A.M. Rutten, Effect of Technological Factors on the Crystallization of Bulk Milk Fat, *Neth. Milk Dairy J. 30*:197–206 (1976).
7. deMan, J.M., Modification of Milk Fat by Removal of a High Melting Glyceride Fraction, *Can. Inst. Food Technol. J. 1*:90–93 (1968).
8. Deffense, E., Milk Fat Fractionation Today: A Review, *J. Am. Oil Chem. Soc. 70*:1193–1201 (1993).
9. Grall, D.S., and R.W. Hartel, Kinetics of Butterfat Crystallization, *Ibid. 69*:741–747 (1992).
10. Kaylegian, K.E., and R.C. Lindsay, Application of Milk Fat Fractions in Foods, in *Handbook of Milkfat Fractionation Technology and Application*, AOCS Press, Champaign, 1995, pp. 525–630.
11. Lund, P., Butterfat Triglycerides, *Milchwissenschaft 43*:159–161 (1988).
12. Breitschuh, B., and E.J. Windhab, Parameters Influencing Cocrystallization and Polymorphism in Milk Fat, *J. Am. Oil Chem. Soc. 75*:897–904 (1998).
13. Herrera, M.L., J.A. Segura, G.J. Rivarola, and M.C. Añón, Relationship Between Cooling Rate and Crystallization Behavior of Hydrogenated Sunflowerseed Oil, *Ibid. 69*:898–905 (1992).

14. Herrera, M.L., Crystallization Behavior of Hydrogenated Sunflower Oil: Kinetics and Polymorphism, *Ibid. 71*:1255–1260 (1994).
15. Gibon, V., P. Blanpain, F. Durant, and C. Deroanne, Application de la Diffraction des Rayons X, de la Resonance Magnetique Nucleaire et de l'Analyse Calorimetrique Differentielle a l'Etude du Polymorphisme et de l'Intersolubilite des Triglycerides PPP, PSP et POP, *Belgian J. Food Chem. Biotechnol. 40*:119–134 (1985).

[Received March 1, 1999; accepted July 30, 2000]